บทความวิจัย

EFFECT OF Lu_2O_3 CONTENT ON RADIATION SHIELDING PROPERTIES OF Lu_2O_3-Na_2O-B_2O_3 GLASSES

Kittisak Sriwongsa[1], Chanin Tinnakorn[2], Supakorn Laoarun[2], Punsak Glumglomchit[3, 5*], Sunantasak Ravangvong[4], Keerati Kirdsiri[5, 6] and Jakrapong Kaewkhao[5, 6]

[1]Lecturers responsible for Bachelor of Education Program in Physics, Faculty of Education, Silpakorn University, Nakhon Pathom, 73000, Thailand

[2]The demonstration school of Silpakorn University, Nakhon Pathom, 73000, Thailand

[3]Huahin Vitthayalai School, Hua–Hin, Prachuap Khiri Khan, 77110, Thailand

[4]Division of Science and Technology, Faculty of Science and Technilogy, Phetchaburi Rajabhat University, Phetchaburi, 76000, Thailand

[5*]Physic Program, Nakhon Pathom Rajabhat University, Nakhon Pathom, 73000, Thailand

[6]Center of Excellence in Glass Technology and Materials Science (CEGM), Nakhon Pathom Rajabhat University, Nakhon Pathom, 73000, Thailand

[*]E-mail: Sriwongsa_k@silpakorn.edu

Received: 2018-09-23
Revised: 2019-01-16
Accepted: 2019-01-30

ABSTRACT

The glasses with composition xLu_2O_3-$20Na_2O$-$(80-x)B_2O_3$, where x = 5, 10, 15 and 20 mol% concentration variations of Lu_2O_3, were measured shielding radiation properties at different photon energies from 1 keV-100 GeV by using WinXCom software program. The values of mass attenuation coefficient, effective atomic number and electron density were found to increase with increasing energy and Lu_2O_3 content. The comparison results of glass systems with ordinary and hematite-serpentine concrete in terms of mass attenuation coefficient, half value layer, mean free bath and Removal cross sections for fast neutrons to test the accuracy of glass systems are about radiation protection. The results indicate that glass systems can be developed as radiation shielding materials.

Keywords: Borate glass, Lutetium, Radiation shielding properties.

Introduction

Due to the increased utilization of gamma rays isotopes in many industries such as nuclear reactors, food irradiation, agriculture, engineering, medical treatment, medical diagnostics, accelerator technologies, and manufacture. These gamma radiations are very damaging not only for personal but include laboratory appliance and environment. To handle with these problems, innovation, and exploration of new effective and feasible radiation shielding material is very important (Chanthima, N., and Kaewkhao, J. 2013, Issa et al., 2017, El-bashir et al., 2017). Concretes are basically used as shielding radiation materials whereas they have many limitations which including; (i) Concretes shielding properties are continuously modified by the escalation of humidity content. (ii) They can't look perpetually concrete because they are not transparent to visible light. (iii) Crack structures occur after exposure to nuclear radiations and prolonged deterioration. (iv) The interaction between nuclear radiations and concrete will cause heat which effects to concretes are a loss of water (Kaur et al., 2014). Glass, once of amorphous materials which normally appropriate properties because of they are an excellent transmission of visible light, easy to modify composition, good transparency, hard and great homogeneity (Kaur et al., 2014, Sayyed, M.I. 2016, El-bashir et al., 2017).

Among many glass materials, B_2O_3 is one of the popular, commonly and excellent glass formers. It can form glass by itself at lower melting points with lower cation size, higher bond strength, good rare-earth ion solubility, thermal stability, high chemical durability, good transparency, and their coordination geometry. It mostly stable configuration in trigonal $[BO_3]^{3+}$ and tetrahedral $[BO_4]^{3+}$ units (Kaur et al., 2012, Singh et al., 2014, Sayyed, M.I., 2016). Sodium-borate glasses have been used wildly as host matrices of lanthanide ions because of their properties, such as good rare-earth ion solubility, high thermal stability, high transparency, and low melting point. Accordingly, Na_2O has been mixed to increase homogenization and reduce melting temperature, of host glass as well as decrease bubbles and breakage (Rajagukguk et al., 2016).

In recent years, research focus on lutetium oxide doped glasses, which have been studied such as luminescent phosphors, single crystal, bioimaging probe, transparent film, up-conversion phosphor, and glass. Lu_2O_3 from RE-O group can be found generally such as energy-saving lamps, color televisions, fluorescent lamps and glasses. It has a highest atomic number of REE (Z = 71), phase stability, low thermal expansion, high melting point and low phonon energy (Locardi et al., 2017, Liqiong et al., 2008, Legendziewicz, J. and Sokolnicki, J., 2008, Faridbod et al., 2015)

Herein, glass systems investigate shielding radiation properties at photon energy from 1 keV-100 GeV of borate glasses contain Lu_2O_3 and Na_2O. In term of HVL and mfp for glass systems are compares with ordinary and hematite–serpentine concrete at photon energy 1 keV-100 GeV.

Methods

A glass systems of Lu_2O_3-Na_2O-B_2O_3 were prepared 4 samples with chemical composition xLu_2O-$20Na_2O$-$(80-x)$ B_2O_3, (x = 5, 10, 15 and 20 mol%), each batch as 10 g. The raw materials H_3BO_3, Lu_2O_3, and Na_2CO_3 were mixed and melted in the electric furnace by melt quenching technic at 1500 °C for 3 h. After that, quickly poured in the block and annealed for 3 h. at 500 °C. In the end, cut and polished the glass systems. Archimedes method was applied to determine the density of the glass systems. A 4-digit sensitive microbalance (A&D, HR-200) was used to investigate the weights of glass systems in air and water, by using the formula ρ (g/cm^3) = (W_a X ρ_b) /(W_a – W_b). While W_a and W_b are weighed the weight of glass systems in air and water respectively, and ρ_b is referred to the density of water at the room temperature (25 °C) that was found to be 1.000 g/cm^3. The shielding radiation properties were measured at different photon energies from 1 keV-100 GeV by using WinXCom software program.

The basic quantities which describe the interaction of gamma rays with shielding radiation mediums are mass attenuation coefficient (μ_m), effective atomic number (Z_{eff}), electron density (N_{el}), mean free path (MFP) and half value layer (HVL) (Chanthima, N., and Kaewkhao, J. 2013,. Sayyed, M.I. 2016). When mono-energetic gamma rays are adapt to a narrow beam and pass into medium, there are interactions between gamma rays photon with the medium. This interaction may be occurred absorbed or scattering of photon. The probability of interactions of photon with the medium can investigate by mass attenuation coefficient (μ_m) in (cm^2/g). For event of mixture or compound of elements, μ_m can be calculated by (Chanthima, N., and Kaewkhao, J., 2013):

$$\mu_m = \sum_i w_i (\mu_m)_i \qquad (1)$$

here wi and $(\mu_m)_i$ are weight fraction and mass attenuation coefficient of element i, respectively. For glass systems, μ_m has been determined by using WinXcom software at energy from 1keV–100 GeV.

The effective atomic number (Z_{eff}) is appropriate quantity for explaining interactions of gamma-ray and can be defined by following (Dong et al., 2017):

$$Z_{eff} = \frac{\sigma_{t,a}}{\sigma_{t,el}} \qquad (2)$$

The total atomic cross-section ($\sigma_{t,a}$) was evaluated by using equation [14]:

$$\sigma_{t,a} = \frac{\mu/\rho}{N_A \sum_i (w_i/A_i)} \qquad (3)$$

here μ, ρ and N_A respectively are linear attenuation coefficient (cm^2/g), the density of the medium (g/cm^3), and Avogadro's number (6.0221415×10^{23} atom/mol).

The total electron cross-section ($\sigma_{t,el}$) of the element can be expressed by (Dong et al., 2017):

$$\sigma_{t,el} = \frac{1}{N_A} \sum_i \frac{f_i A_i}{Z_i} (\mu/\rho)_i \qquad (4)$$

here Z_i and f_i denoted atomic number and fractional abundance of mixture element i, respectively.

The electron density (N_{el}) is the number of electrons per unit mass and calculated by (Chanthima, N. et al., 2017):

$$N_{el} = (\mu/\rho)/(\sigma_{t,el}) \qquad (5)$$

The half value layer (HVL) is thickness of medium which reduces photon intensity to half of the incident intensity (I_0), and computed by using formula (Kaur et al., 2016):

$$HVL = \frac{0.693}{\mu} \qquad (6)$$

Mean free path (MFP) is the average distance between two successive interactions is given by (Chanthima, N., and Kaewkhao, J., 2013):

$$MFP = \frac{1}{\mu} \quad (7)$$

Furthermore, effective removal cross–section for compounds and homogeneous mixtures can be computed from value Σ_R (in cm^{-1}) or $\Sigma_{R/\rho}$ (in cm^2/g) for various elements in compounds or mixtures by using formula (Singh et al., 2014):

$$\Sigma_R = \sum_i \rho i \, (\Sigma_R/\rho)_i \quad (8)$$

here ρ_i is partial density and $\Sigma_{R/\rho}$ is mass removal cross–section of ith constituent. $\Sigma_{R/\rho}$ values of elements apply from Kaplan and Chilton (Singh et al., 2014).

Results and discussion

This work, glass systems which varied Lu_2O_3 at 5, 10, 15 and 20 mol% content were melted by quenching technique and all glass samples are good transparency which exhibited in Fig.1. Density is tool in indicating the degree of adjusting information with remodeling in glass composition in order to know molecular packing inside medium (Mohd Zaid et al., 2016). Densities of glass systems were applied Archimedes technique and shown in Table 1. From Table 1 density of glass, system was increased with increasing Lu_2O_3 content that because of replacing of B_2O_3 by Lu_2O_3 which Lu_2O_3 has a molecular weight higher than B_2O_3.

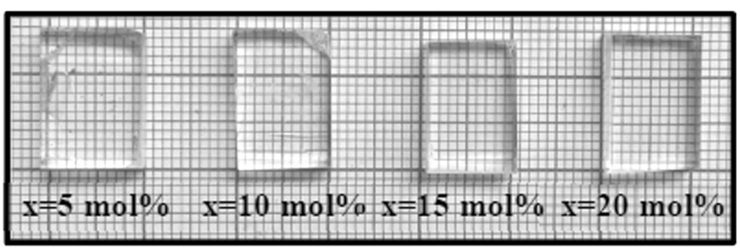

Figure 1 Photograph of Lu2O3 based glass systems

Table 1: Chemical compositions of the glass systems (mol%)

$[Lu_2O_3]$ (mol%)	Glass samples	Density (g/cm^3)
5	$5Lu_2O_3:20Na_2O:75B_2O_3$	2.7090 ± 0.0015
10	$10Lu_2O_3:20Na_2O:70B_2O_3$	3.1593 ± 0.0034
15	$15Lu_2O_3:20Na_2O:65B_2O_3$	3.3981 ± 0.0012
20	$20Lu_2O_3:20Na_2O:60B_2O_3$	3.7946 ± 0.0023

1. Mass attenuation coefficients

The variation of μ_m with energy from 1 keV-100 GeV for glass systems is exhibited in **Figure 2**

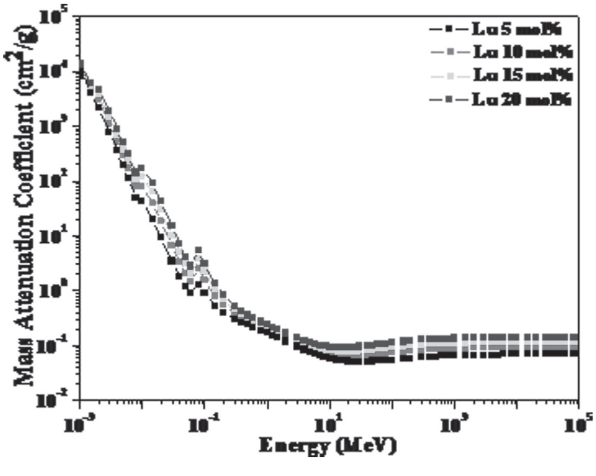

Figure 2 μ_m of glass systems with energy from 1 keV-100 GeV

Clearly, from **Figure 2,** μ_m for glass systems, decrease exponentially with the increase of photon energy. It is noted that, at low energy range (E < 500 keV), μ_m values of glass systems are very large and decrease rapidly with increasing energy. So, in this energy range, μ_m values were discontinuities due to absorption edge of lutetium at M (M_5: 1.588 X 10^{-3} MeV, M_4: 1.639 X 10^{-3} MeV, M_3: 2.024 X 10^{-3} MeV, M_2: 2.263 X 10^{-3} MeV, M_1: 2.491 X 10^{-3} MeV), L (L_3: 9.244 X 10^{-3} MeV, L_2: 1.035 X 10^{-2} MeV, L_1: 1.087 X 10^{-1} MeV) and K (6.331 X 10^{-2} MeV) energy level and absorption edge of sodium K (1.072 X 10^{-3} MeV) energy level. In intermediate energy range (500 keV < E < 1 MeV), μ_m values decrease at slower rate, while for E > 1 MeV, μ_m values become nearly constant with increase of energy. These variations in μ_m values can be discussed by applying three partial photon interactions with the medium. The photoelectric effect and pair production processes appearing at lower and higher energy range. For intermediate energy range, Compton scattering process is the main interaction process. It is noted that μ_m values increase with increment in Lu_2O_3 concentration in glass systems. From Figure 2 μ_m values for glass sample with 20 mol% Lu_2O_3 are largest in glass systems; hence, this sample is excellent gamma ray shielding glasses.

2. Effective atomic number and electron density

The variation of Z_{eff} and N_{el} with energy for glass systems has been exhibited in Figure 3 and 4, respectively. Z_{eff} values for glass systems increases with increasing of energy. From Figure 3, Z_{eff} values acute shift occurs at 15 keV and 80 keV that can be discussed on knowledge of K edge absorption of Lu and Na respectively. Whereas, for glass systems at energies ranging from 80 keV-500 keV, Z_{eff} rapid decrease with increasing energy which can be discussed on basic of the dependence of cross–section of photoelectric effect which varies inversely with photon energy as $E^{3.5}$. Besides, glass systems at energy range from 0.5-7.0 MeV, Z_{eff} values are nearly independent of energy. That may be because of Compton scattering is the main process. At energy increases over 7.0 MeV, Z_{eff} values increases slowly and starts nearly constant over 80 MeV. That can discuss base on of pair production is dominance in higher energy range.

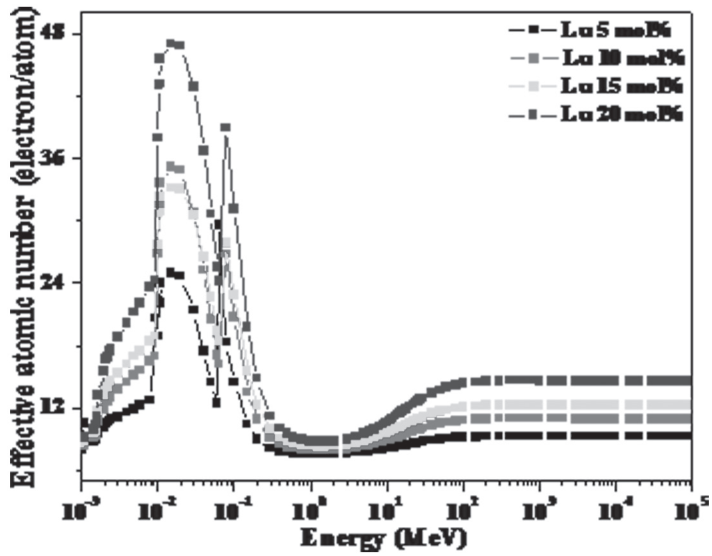

Figure 3 Z_{eff} of glass systems with energy from 1 keV-100 GeV

Figure 4 the variation of N_{el} with energy, in the range 1 keV-100 GeV, has indicated identical behavior of Z_{eff}.

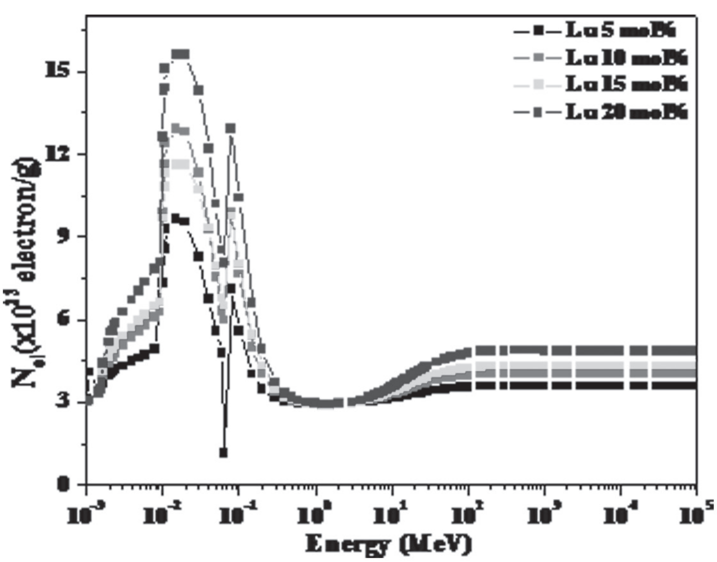

Figure 4 N_{el} of glass systems with energy from 1 keV-100 GeV

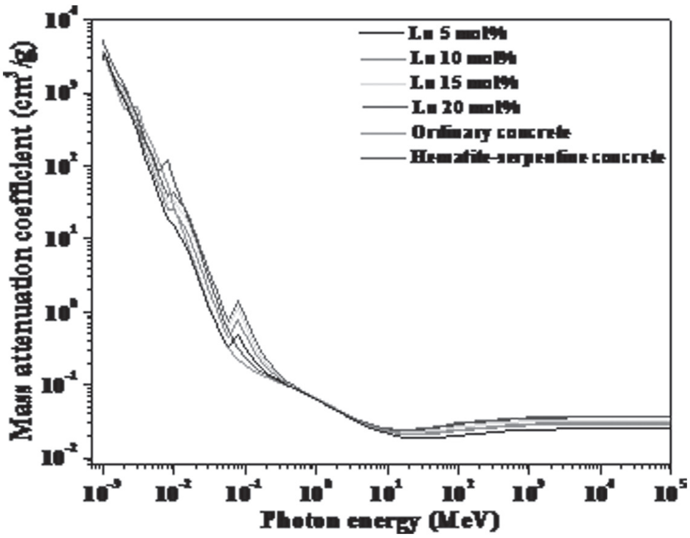

Figure 5 μ_m of glass systems, ordinary and hematite serpentine concrete with energy from 1 keV-100 GeV

Figure 5 exhibits μ_m of glass systems compared with ordinary and hematite-serpentine concrete (Bashter, I.I., 1997). From Fig. 5, μ_m of glass systems had a little higher values compared with some standard concrete mentioned earlier at intermediate energy range where Compton scattering is the main process.

3. Half-value layer and mean free path

The half value layer (HVL) is the parameter to describe radiation attenuation for the medium which medium has lower HVL values that are indicated better radiation shielding. Figure 6 exhibited results of comparison for glass systems with ordinary and hematite-serpentine concrete (Bashter, I.I., 1997).

From Figure 6, HVL values of glass systems increases up to 10 MeV and start nearly constant with increasing energy. The effect of increasing Lu_2O_3 content, HVL of glass systems were decreased that indicted gamma-ray shielding improves with the increment of Lu_2O_3 content. In part of comparison HVL, glass samples contained Lu_2O_3 at 10, 15 and 20 mol% have lower HVL values than ordinary and hematite-serpentine concrete. At energy lower 40 MeV, glass sample contained Lu_2O_3 at 5 mol% has HVL values lower than ordinary concrete after that it has HVL values higher than.

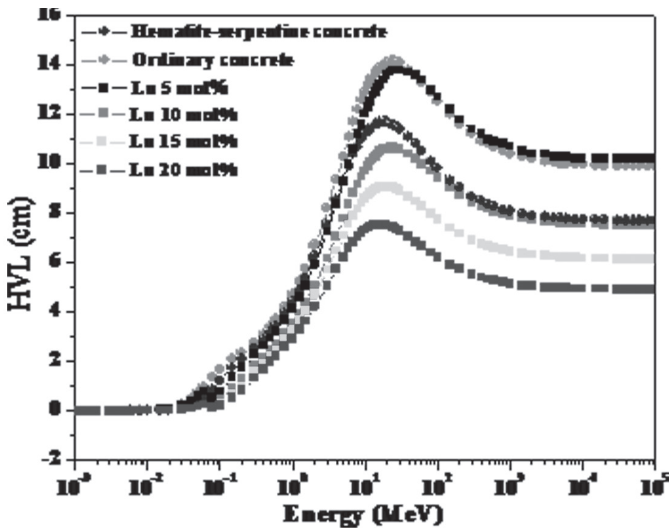

Figure 6 HVL of glass systems, ordinary and hematite-serpentine concrete with energy from 1 keV-100 GeV

The comparison means free path (mfp) values for glass systems, ordinary and hematite-serpentine concrete are exhibited in Fig. 7. From the figure, glass samples contained Lu_2O_3 at 10, 15 and 20 mol% have lower MFP values than all mentioned concretes. For glass contained Lu_2O_3 at 5 mol% at energy lower 40 MeV has MFP values lower than ordinary concrete after that it has MFP values higher than. So glass systems ability to be applied as the radiation shielding material.

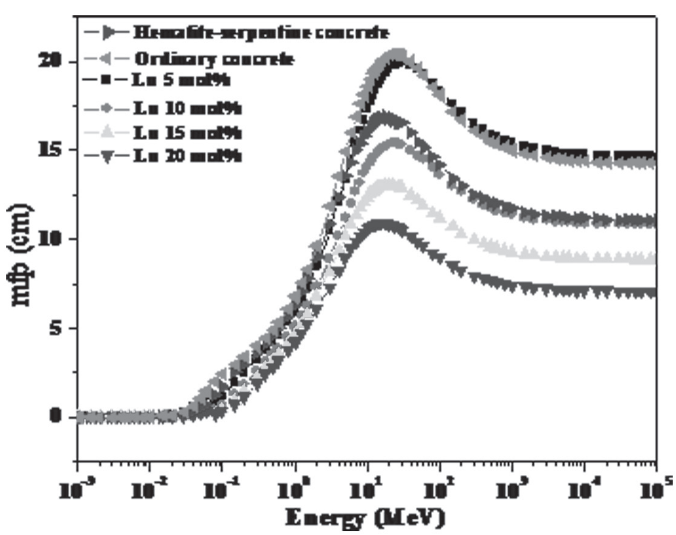

Figure 7 MFP of glass systems, ordinary and hematite serpentine concrete with energy from 1 keV-100 GeV

4. Removal cross-section for fast neutron

Table 2 Removal cross sections for fast neutrons Σ_R (cm^{-1}) for glass systems, ordinary and hematite-serpentine concrete.

Sample	Σ_R (cm^{-1})	Reference
$5Lu_2O_3$:$20Na_2O$:$75B_2O_3$	0.1144	This work
$10Lu_2O_3$:$20Na_2O$:$70B_2O_3$	0.1285	This work
$15Lu_2O_3$:$20Na_2O$:$65B_2O_3$	0.1329	This work
$20Lu_2O_3$:$20Na_2O$:$60B_2O_3$	0.1425	This work
Ordinary concrete	0.0937	[17]
Hematite-serpentine concrete	0.0967	[17]

The removal cross-section for fast neutron (Σ_R) for glass systems is exhibited in Table 2. It was found that Σ_R values for glass systems increase with the increase in Lu_2O_3 content. This result occurs replacement of B_2O_3 by Lu_2O_3 and Σ_R for glass systems found higher than ordinary and hematite–serpentine concrete.

Conclusions

In this work, density of glass systems was increased with increasing Lu2O3 content. The values of μ_m, Z_{eff}, N_{el}, HVL, and MFP for glass systems were measured for total photon interaction by using WinXCom software program at energy range from 1 keV-100 GeV. The values of μ_m, Z_{eff} and N_{el} were found to increase with increasing energy and Lu_2O_3 content. The comparison results of glass systems with ordinary and hematite-serpentine concrete in terms of μ_m, HVL, MFP, and Σ_R to test the accuracy of these glass systems are about radiation protection. Glass systems can be developed for radiation shielding materials.

Acknowledgement

The financial support from Nakhon Pathom Rajabhat University is gratefully acknowledged.

References

An, Liqiong., Zhang, Jian., Liu, Min. & Wang, Shiwei. (2008). Upconversion luminescence of Tm^{3+} and Yb^{3+}–codoped lutetium oxide nanopowders. **Journal of Alloys and Compounds.** 451, 538–541.

Bashter, I.I. (1997). Calculation of radiation attenuation coefficients for shielding concretes. **Annals of Nuclear Energy.** 24, 1389–1401.

Chanthima, N., and Kaewkhao, J. (2013). Investigation on radiation shielding parameters of bismuth borosilicate glass from 1 keV to 100 GeV. **Annals of Nuclear Energy.** 55, 23–28.

Chanthima, N., Kaewkhao, J., Limkitjaroenporn, P., Tuscharoen, S., Kothan, S., Tungjai, M., Kaewjaeng, S., Arachai, S. & Limsuwan, P. (2017). Development of BaO–ZnO–B_2O_3 glasses as a radiation shielding material. **Radiation Physics and Chemistry.** 137, 72–77.

Dong, M.G., Sayyed, M.I., Lakshminarayana, G., Çelikbilek Ersundu, M., Ersundu, A.E., Nayar, Priyanka. & Mahdi, M.A. (2017). Investigation of gamma radiation shielding properties of lithium zinc bismuth borate glasses using XCOM program and MCNP5 code. **Journal of Non-Crystalline Solids.** 468, 12–16.

El-bashir, B.O., Sayyed, M.I., Zaid, M.H.M. & Matori, K.A. (2017). Comprehensive study on physical, elastic and shielding properties of ternary BaO–Bi_2O_3–P_2O_5 glasses as a potent radiation shielding material. **Journal of Alloys and Compounds.** 708, 294–300.

Faridbod, F., Sedaghat, M., Hosseini, M., Ganjali, M.R., Khoobi, M., Shafiee, A. & Norouzi, P. (2015). Turn–on fluorescent chemosensor for determination of lutetium ion. **Spectrochimica Acta Part A: Molecular and Biomolecular.** 137, 1231–1234.

Issa, Shams A.M. & Mostafa, A.M.A. (2017). Effect of Bi_2O_3 in borate–tellurite-silicate glass system for development of gamma–rays shielding materials. **Journal of Alloys and Compounds.** 695, 302–310.

Kaur, Gurbinder., Pandey, O.P. & Singh, K. (2012). Effect of modifiers field strength on optical, structural and mechanical properties of lanthanum borosilicate glasses. **Journal of Non-Crystalline Solids.** 358, 2589–2596.

Kaur, Sandeep. & Singh, K.J. (2014). Investigation of lead borate glasses doped with aluminium oxide as gamma ray shielding materials. **Annals of Nuclear Energy.** 63, 350–354.

Kaur, Kulwinder., Singh, K.J. & Anand, Vikas. (2016). Structural properties of Bi_2O_3–B_2O_3–SiO_2–Na_2O glasses for gamma ray shielding applications. **Radiation Physics and Chemistry.** 120, 63–72.

Legendziewicz, J. & Sokolnicki, J. (2008). Spectroscopy and structural characteristic of Yb^{3+} and Nd^{3+} ions doped nanostructured Lu_2O_3 and sol–gel derived silica host materials. **Journal of Alloys and Compounds.** 451, 600–605.

Locardi, F., Gianotti, E., Nelli, I., Caratto, V., Martinelli, A., Ferretti, M., Costa, G.A., Canesi, L., Balbi, T., Fasoli, M., Martini, M., Estevão, B.M. & Miletto, I. (2017). Facile synthesis of NIR and Visible luminescent Sm^{3+} doped lutetium oxide nanoparticles. **Materials Research Bulletin.** 86, pp. 220–227.

Mohd Zaid, Mohd Hafizd., Matori, Khamirul Amini., Ab Aziz, Sidek Hj., Kamari, Halimah Mohamed., AbdulWahab, Zaidan., Effendy, Nuraidayani. & Alibe, Ibrahim Mustapha. (2016). Comprehensive study on compositional dependence of optical band gap in zinc soda lime silica glass system for optoelectronic applications. **Journal of Non-Crystalline Solids.** 449, 107–112.

Sayyed, M.I. (2016). Bismuth modified shielding properties of zinc boro–tellurite glasses. J. **Alloys Compds.** 688, 111-117.

Singh, Vishwanath P., Badiger, N.M. & Kaewkhao, J. (2014). Radiation shielding competence of silicate and borate heavy metal oxide glasses: Comparative study. **Journal of Non-Crystalline Solids.** 404, 167–173.

Rajagukguk, J., Kaewkhao, J., Djamal, M., Hidayat, R., Suprijadi & Ruangtaweep, Y. (2016). Structural and optical characteristics of Eu^{3+} ions in sodium–leadzinc–lithium–borate glass system. **Journal of Molecular Structure.** 1121, 180–187.